Structure and Properties of Neat Liquids Using Nonadditive Molecular Dynamics: Water, Methanol, and *N*-Methylacetamide

James W. Caldwell and Peter A. Kollman*

Department of Pharmaceutical Chemistry, University of California, San Francisco, California 94143-0446

Received: October 4, 1994; In Final Form: February 2, 1995[⊗]

We present the first nonadditive molecular dynamics simulation of organic liquids, studying the structure and energetics of methanol and N-methylacetamide. Beginning with an additive potential that reproduces the structure and energetics of these liquids quite well, we have shown that one can simply reduce the atomic charges by a scale factor in the range of 0.88−0.90 and add isotropic atomic polarizabilities to create nonadditive models that also quite accurately reproduce the structures and energies of these liquids. Thus, we have a clear pathway for the general inclusion of nonadditive effects for organic and biological molecules.

Introduction

Force field/molecular mechanics methods are proving to be very useful and powerful in the study of condensed phase systems. They can complement and often go beyond experiment in the molecular detail and insight that they offer. However, given their approximate nature and general application within the context of classical rather than quantum mechanics, it is essential that the results emerging from them be checked against experiment as often as possible. The philosophy of the OPLS model[1] illustrates this, in that it has been carefully calibrated to reproduce the density and enthalpy of vaporization of organic liquids, and then these parameters have been successfully used in studies of heterogeneous systems. The OPLS model for intermolecular interactions has also been combined with the intramolecular parameters of Weiner *et al.*[2] to derive a force field for peptides and proteins[1a] that has proven useful in studying such systems.

We have been developing a "second-generation" force field[3] to follow up the efforts of Weiner *et al.*[2] and agree with the OPLS approach on the usefulness of studying organic liquids to help in devising and assessing force field parameters. For example, we have carried out Monte Carlo simulations on liquid hydrocarbons to derive all atom van der Waals parameters for aliphatic carbons and hydrogens bonded to carbon[4] and used molecular dynamics on CF_4 and CHF_3 to derive van der Waals parameters for fluorine and hydrogens in various bonding environments.[5] Many of our differences with the OPLS method are only in the small details, but the major one is our conviction that the atomic partial charges for the model should come from quantum mechanical calculations[6] rather than experiment. This conviction is based both on the view that such a model is more general and generalizable than a purely empirical approach to deriving charges[7] and on the lucky/fortuitous properties of the 6-31G* basis set.

Empirical charge models of polar liquids automatically include inherent polarization of the molecules relative to their gas phase charge distribution in an average way. Thus, they lead to charge distributions for molecules with dipole moments enhanced over gas phase values. The 6-31G* basis set enhances polarity by about the same magnitude relative to gas phase moments as does the OPLS[1] model. Hence, charges derived by fitting to the electrostatic potential using a 6-31G* basis set should lead to reasonable models for partial charges for molecules. Some support of this comes from the very good representation of the relative free energies of benzene, anisole, and trimethoxybenzene[8] calculated using such a model. The development of RESP (restrained electrostatic potential) model has been an important improvement over the standard approach to the derivation of charges using electrostatic potentials, in that it offers improvement in the treatment of intramolecular properties while retaining the good description of intermolecular interactions.[9,10] A key guidepost in the development of the RESP model was the reproduction of the aqueous free energy of solvation of methanol (MEOH) and *N*-methylacetamide (NMA) in TIP3P water. This involved extensive testing of which van der Waals parameters were appropriate to use with these charges. The detailed description of these are given below.

However, calculating $\Delta G_{solvation}$ in good agreement with experiment is only a single test of a model; the calculation of the density and enthalpy of the molecular liquids is a more challenging test. Thus, a first goal of this paper is to present the results of liquid simulations on methanol and *N*-methylacetamide using the same effective two-body additive potential used in the solvation free energy calculations and to compare to experiment.

It is, however, clear that effective two-body potentials have limitations. These limitations would be expected to be most severe for molecules of high charge/polarity at interfaces, since in these cases, the assumption of a single "average polarized" charge distribution for the molecule would be least accurate. We have developed a nonadditive model for water[11a] that reduces the partial charges of the atoms and adds isotropic atomic polarizabilities resulting in a similarly accurate description of the liquid compared to two-body additive models. A study of ion−water clusters with such a model led to new and interesting insights into their structure and energetics.[11b] However, to prove the utility and generality of such nonadditive models, they must be extended to more complex molecules. Thus, the second goal of this study is to apply the same approach to deriving the nonadditive model for water to the more complex molecules methanol and *N*-methylacetamide.

Encouragingly, both the additive and nonadditive models, with very similar electrostatic scale factors for all three molecules (to derive charges for the nonadditive models), lead to good agreement with experimental densities and enthalpies of vaporization.

[⊗] Abstract published in *Advance ACS Abstracts,* March 15, 1995.

0022-3654/95/2099-6208$09.00/0

There have been a number of different approaches to treat nonadditivity in liquid water including the one we have developed,[11a] the (polarizable SPC) model of Ahlstom *et al.*,[12a] the ("anisotropic" water) model of Levy and co-workers,[12b] the model of Dang[12c] (which is a modification of the model in ref 11a), the microcharge model of Sprik and Klein,[12d] and the "flowing charge" model of Rick *et al.*[12e] Models in refs 11a and 12a–c have common parentage and are straightforward to generalize to complex systems. The approaches of Sprik and Klein[12d] and Rick *et al.*[12e] are computationally more efficient, but it is not clear how to generalize them beyond simple liquids.

Computational Methods

The molecular mechanical energy[2] was calculated using the following energy equations:

$$E_{\text{total}} = \sum_{\text{bonds}} K_r(r - r_{\text{eq}})^2 + \sum_{\text{angles}} K_\theta(\theta - \theta_{\text{eq}})^2 + \sum_{\text{dihedrals}} \frac{V_n}{2}[1 + \cos(n\phi - \gamma)] + \sum_{i<j}^{\text{atoms}} \left[\frac{A_{ij}}{R_{ij}^{12}} - \frac{B_{ij}}{R_{ij}^{6}} + \frac{q_i q_j}{\epsilon R_{ij}}\right]$$

with the nonadditive[11] contribution included via

$$-\frac{1}{2}\sum_{i}^{\text{atoms}} (\vec{\mu}_i \cdot \vec{E}_i^{\,0}) \tag{1}$$

where

$$\vec{\mu}_i = \alpha_i \vec{E}_i \tag{2}$$

$$\vec{E}_i = \vec{E}_i^{\,0} + \sum_{i=1_{j\neq i}} T_{ij}\vec{\mu}_j \tag{3}$$

$$E_i^{\,0} = \sum_{j=1_{j\neq i}} q_j \frac{\vec{r}_{ij}}{r_{ij}^{\,3}} \tag{4}$$

$$T_{ij} = \frac{1}{r_{ij}}\left(3\vec{r}_{ij}\left(\frac{\vec{r}_{ij}}{r_{ij}^{\,2}}\right) - 1\right) \tag{5}$$

The meaning of the parameters is described in refs 2 and 11.

In the original approach of Applequist, all atom–atom interactions (i.e. charge and inducible dipoles) were considered.[13] This approach is also taken by Thole.[14] We have chosen to follow the algorithm of the standard molecular mechanics approah to through-space interactions[2] and only include interactions of nonbonded and 1–X bonded interactions, where $X > 3$ (the 1–2 and 1–3 charge–charge and vdw–vdw interactions are folded into the bond and angle force constants). While this will make calculation of the total molecular polarizability inaccurate using existing parameters (e.g. Applequist's values[13]), that quantity is only peripheral to our work. We are mainly interested in the energetics of molecular interactions. The approach taken will also allow efficient computation of the nonadditive interactions using the standard nonbond pair list from additive molecular mechanics; it also has the advantage that the potential for a polarization catastrophe (polarization energy becoming unrealistically large) is reduced.

Also, given all the other approximations used to represent the noncovalent interactions between molecules with eq 1, using the Applequist data within the context of this equation is certainly reasonable. We also found that with such an approach centering the entire molecular polarizability of water ($\alpha = 1.44$ Å^3) on the oxygen or distributing it to the oxygens and hydrogens leads to too large $Na^+\cdots OH_2$ interactions.[11a] Using the Applequist atomic polarizabilities on the oxygen and hydrogen directly and varying the atomic partial charges on water leads to excellent representations of both water liquid and ion–water clusters. We thus have proceeded to develop this model.

The OPLS results of Jorgensen include a long-range correction to approximately include the average van der Waals effect of the molecules that are outside the spherical cutoff. This term should make only a small difference in the total energy and density. This was borne out by the calculations discussed below.

Water. The hydrogen was assigned a van der Waals term of 0 and all the other interactions were of the 6–12 form, following the approach of Jorgensen's OPLS[1,15] models for liquids. The polarizabilities are those proposed by Dang[12c] to correctly reproduce the molecular polarizability (we feel that water's unique role in nature merits special attention to detail). The charges were those of the previous POL1 model. We performed a series of molecular dynamics runs varying r^* and ϵ on a system of 216 molecules of water in a cubic box. Constant temperature (300 K) and pressure (1 bar) were maintained by coupling the system to temperature and pressure baths[16] with coupling parameters $\tau_T = 0.4$ ps and $\tau_P = 0.4$ ps. The SHAKE[17] algorithm was used to maintain constant bond lengths. The total time was 100+ ps, although the properties of water tend to converge very quickly (~10 ps). The goal here was to derive optimal liquid properties for this model (POL3); final values of r^* and ϵ are given in Table 1. They are very similar to those used previous,[11] including the use of the SPC/E geometry.[18]

Methanol and *N*-Methylacetamide. The force field parameters for the additive model[10] are presented in Table 1. The basis of the calculation was the new Cornell *et al.* force field,[3] wherein the 1–4 electrostatic scale term is now 1.2 as opposed the value of 2.0 used previously.[2] The additive model atomic partial charges were the RESP[9] charges determined using the 6-31G* basis set in Gaussian 92.[19] The atomic (isotropic) polarizabilities are those developed by Applequist.[12]

A comparison of the experimental, quantum mechanical, and molecular mechanical dipole moments appears in Table 2. It is apparent that the nonadditive part of the molecular mechanical Hamiltonian is crucial in providing good liquid dipole moments for water and *N*-methylacetamide.

The simulation scheme was the same as for water: periodic boundary conditions, constant temperature (300 K for MEOH and 373 K for NMA), and constant pressure (1 bar). A time step of 1 fs (2 fs for additive models) and a pair list update every 5–10 molecular dynamics steps were used. The nonbond cutoff was set at 8.0 Å for methanol and 10.0 Å for NMA. NMA is the largest of the systems; it takes a considerable amount of computer time: 4 cpu-hours/ps on a DEC 3000/500 or HP 9000/735-99.

The $\Delta H_{\text{vaporization}}$ was determined via the scheme

$$E_{\text{monomer}}(T) = E_{\text{minimized}} + E_{\text{vibrational}}(T)$$

where

$$E_{\text{vibrational}} = RT(3N - 6 - (\text{shaken bonds}))/2$$

with all bonds shaken[16] for both MEOH and NMA. And

$$\Delta E = E_{\text{potential-system}} - N_{\text{monomers}}E_{\text{monomer}}$$

$$\Delta H = \Delta E + \Delta nRT$$

In order to calculate quadrupole moments, we represented the

TABLE 1: Force Field Parameters for Methanol and *N*-Methylacetamide

Van der Waals Parameters

atom type	r^{*a}	ϵ^a	α^a
	Water		
HW	0.0	0.0	0.170
OW	1.7980	0.156	0.528
	MeOH		
CT	1.9080	0.1094	0.878
HO	0.0	0.0	0.135
HC	1.3870	0.0157	0.135
OH	1.7210	0.2104	0.465
	NMA		
C	1.9080	0.0860	0.616
CT	1.9080	0.1094	0.878
HN	0.6000	0.0150	0.161
H1	1.4870	0.0150	0.135
H2	1.3870	0.0150	0.135
N	1.8240	0.1700	0.530
O	1.7683	0.1520	0.434

atom	atom type	charge[b]
	Water	
H	HW	0.3650
O	OW	−0.7300
	MeOH	
HC	HC	0.0372
C	CT	0.1166
OH	OH	−0.6497
HO	HO	0.4215
	NMA	
H1	H1	0.0173
H2	H1	0.0173
H3	H1	0.0173
C1	CT	−0.0411
C	C	0.5869
O	O	−0.5911
N	N	−0.4192
HN	H	0.2823
C2	CT	−0.2078
H4	H2	0.1127
H5	H2	0.1127
H6	H2	0.1127

bonds[c]	K	R_{eq}	bonds[c]	K	R_{eq}
C−CT	317.0	1.522	CT−H2	340.0	1.098
C−N	490.0	1.335	CT−N	337.0	1.449
C−O	570.0	1.229	CT−OH	320.0	1.41
CT−HC	340.0	1.098	N−HN	434.0	1.01
CT−H1	340.0	1.098			

angle[d]	K_θ	θ_{eq}	angle[d]	K_θ	θ_{eq}
C−N−HH	35.0	119.8	H1−CT−H1	35.0	109.5
C−N−CT	50.0	121.9	H2−CT−H2	35.0	109.5
CT−C−N	70.0	116.6	H1−CT−C	50.0	109.5
CT−C−O	80.0	120.4	H2−CT−N	50.0	109.5
CT−OH−HO	55.0	108.0	H−N−CT	50.0	120.0
HC−CT−HC	35.0	109.5	N−C−O	80.0	122.9
HC−CT−OH	35.0	109.5			

dihedral[e]	redundancy[f]	$V_n/2^e$	γ^e	n^e
X−CT−N−X	6	0.0	0.0	3
X−C−N−X	4	10.0	180.0	2
X−CT−OH−X	3	0.5	0.0	3
H−N−C−O	1	2.5	180.0	2
H−N−C−O	1	2.0	0.0	1
H1−CT−C−O	1	0.067	180.0	3

improper dihedral[e]	$V_n/2^e$	γ^e	n^e
X−X−N−H	1.0	180.0	2
X−X−C−O	10.5	180.0	2

[a] r^* in Å, ϵ in kcal/mol, α in Å^3. [b] Atomic units. [c] K_R in kcal/(mol Å^2). R_{eq} in Å. [d] K_θ in kcal/(mol radians^2). θ_{eq} in degrees. [e] $V_n/2$ in kcal/mol, γ is the phase offset in degrees, n is the periodicity of the Fourier term. [f] The redundancy is determined for X−A−B−X as the product of the number of X−A bonds with the number of B−X bonds.

TABLE 2: Dipole Moments for Isolated Molecules (D)

	exptl	qm[a,b]	mm (add[b])	mm (nonadd[b])
water	1.85[b](2.6[c])	2.20	2.35	2.02/−/2.02[d]
methanol	1.69	1.89	2.16	1.90/0.10/1.93[d]
NMA	3.7[e]	3.91	4.45	3.88/0.621/3.35[d]

[a] 6-31G* optimized geometries. [b] Gas phase. [c] Liquid, ref 21. [d] Permanent moment/induced moment/vector sum. [e] Average of 3.71 (gas phase), 3.82 (in benzene), and 3.6 (in CCl_4), ref 30.

TABLE 3: Water Energetics (T = 300 K, P = 1 bar)

Liquid

	density[a]	ΔE^b
exptl[c]	0.995	9.92
SPC/E	0.997	9.90
POL3	0.998	9.83

Dimers

	SPC/E	POL3
$E_{minimized}$[b,d]	−7.13	−5.45
R_{H-O}[e]	1.79	1.86
R_{O-O}[e]	2.78	2.85

[a] gm/cm^3. [b] kcal/mol. [c] See ref 14. [d] Total molecular mechanical energy, which is also the dimerization energy since the monomer energy is 0.0 for rigid water models. [e] Å.

quadrupole moment contributions due to the induced dipoles by microdipoles. These were determined by treating the induced dipoles as comprised of pseudocharges separated by a sufficient distance to produce a dipole moment the same as the induced one. (We found that charges of $\pm 16e$ mimicked the infinitesimal induced moments (we tested values from $0.5e$ to $64e$).)

Results

Scale Factors. The charges originally used for POL1 water[11] were used in this work since they had been shown to give a reasonable value of the gas phase monomer dipole moment and also to yield a good bulk dipole moment. The value which best covered these two disparate environments is 0.86 of the additive (SPC/E) value.[18]

The criterion used in the MEOH and NMA simulations was rather different: find a scale factor which would give the same bulk properties with polarization switched on as the additive model. The consensus value is found to be 0.88.

Water. For our simulations, we were aiming at experimental values of $\Delta H_{vaporization}$ = 10.51 kcal/mol and density = 0.995 gm/cm.[3] The "best" values were found to be r^* = 1.798 and ϵ = 0.156, which yield a ΔH 10.42 kcal/mol and 0.998 gm/cm.[3] The calculated dipole moment is 2.61 D, nearly the presumed experimental value (~2.6 D)[20] (Tables 2 and 3). The radial distribution functions are compared to experiment[21] in Figures 1−3, where it is seen that agreement is good, although the first O−O peak is somewhat at too short a distance (which is typical of models proposed thus far[14]). The agreement with SPC/E is very good (Figure 4). However, we cannot obtain the previously published value (0.25×10^{-8} m^2/s) of the diffusion constant for SPC/E, even extending our calculation to 1.5 ns (the published work only determined the diffusion constant for 20 ps). Both POL3 and SPC/E yield values of 0.31×10^{-8} m^2/s, which is somewhat high compared with the experimental value[22] of 0.23×10^{-8} m^2/s (Figure 5). The calculated quadrupole moment (Table 4) is smaller than the quantum mechanical value,[23] reflecting the inherent inability of three-point models to reproduce both the dipole and quadrupole moments.

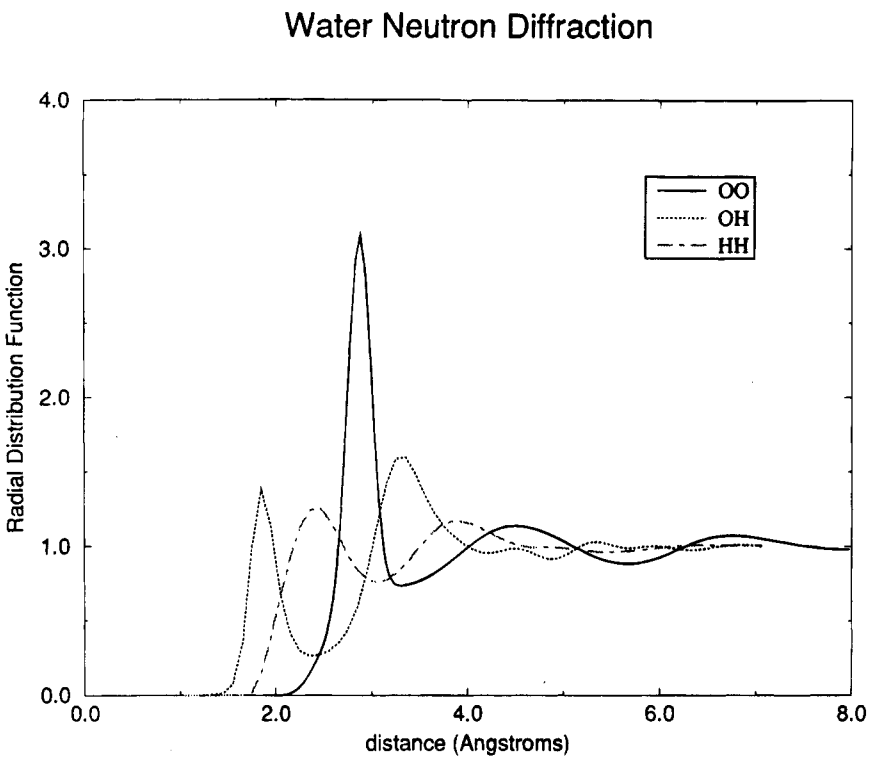

Figure 1. Water neutron diffraction radial distribution functions from data in ref 18.

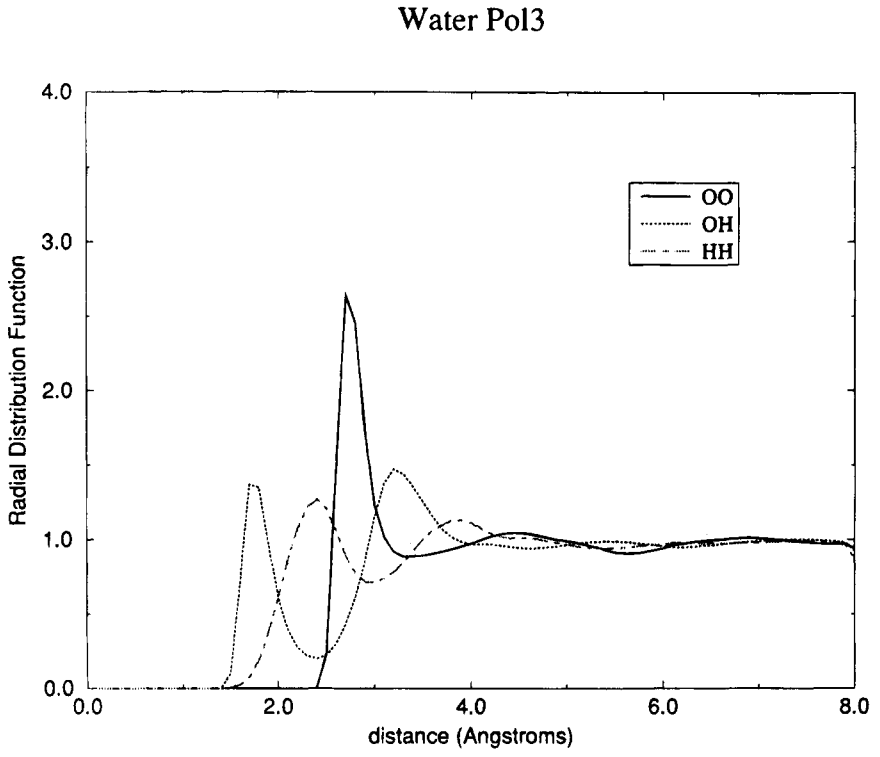

Figure 2. Water: POL3 radial distribution functions (T = 300 K, P = 1 bar, 216 molecules/box, >20 000 step average).

Methanol. The energy components of monomeric and dimeric methanol for both polarizable and additive models are presented in Table 5. The dimerization energy is seen to be −5.6 kcal/mol for the additive model and −5.4 kcal/mol for the nonadditive model. Earlier work of Jorgensen found an average dimerization energy of −4.4 kcal/mol for his rigid model.[24b]

The liquid simulations were run for very long trajectories, the additive simulation was run for 2+ ns (including testing simulation protocols as well), and the nonadditive was run for 350+ ps (the nonadditive model model runs about 4× slower than the additive). The energetics of the current calculation are shown in Table 5 and the radial distribution functions (RDFs) in Figures 6 and 7. The calculated $\Delta H_{\text{vaporization}}$ is 8.45 kcal/mol for the additive model and 9.05 kcal/mol for the nonadditive model using a scaling factor of 0.88 for the partial charges; the experimental $\Delta H_{\text{vaporization}}$ is ~9.0 kcal/mol.[20] The densities are 0.775 and 0.820 gm/cm^3, respectively, as compared to an experimental value[25] of 0.787 gm/cm^3. While the nonadditive $\Delta H_{\text{vaporization}}$ is quite good, the system is somewhat too dense.

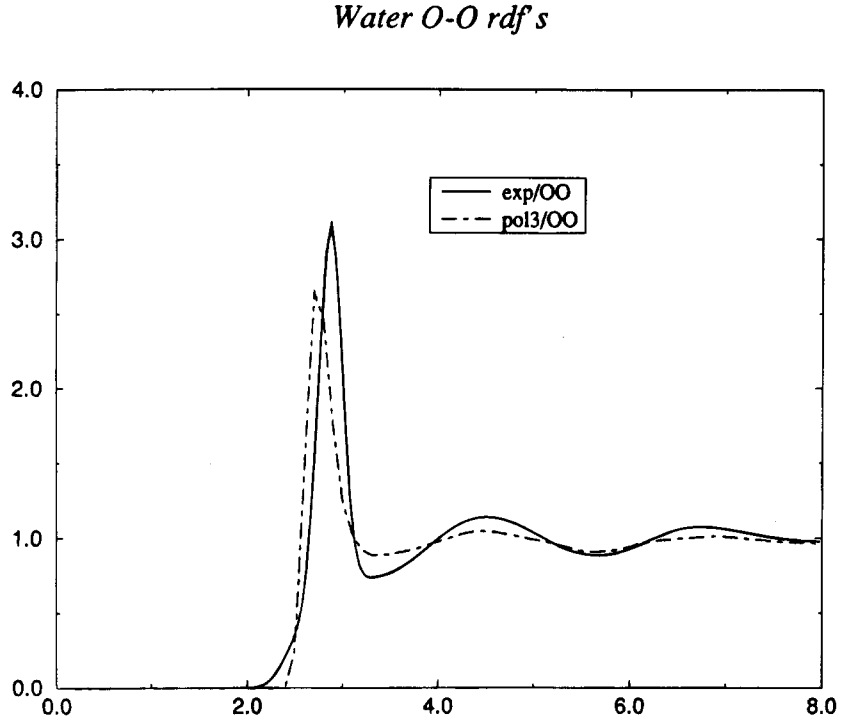

Figure 3. Water: comparison of the experimental and calculated oxygen–oxygen radial distribution functions (T = 300 K, P = 1 bar, 216 molecules/box, >20 000 step average).

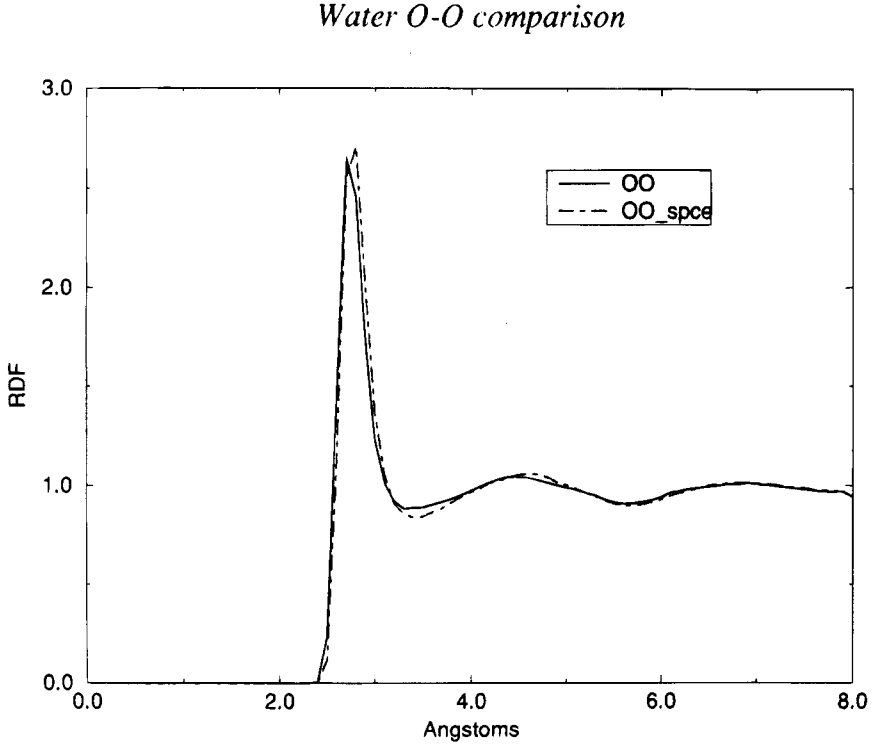

Figure 4. Water: comparison of SPC/E and POL3 O–O radial distribution functions.

(The OPLS values[24] are $\Delta H_{\text{vaporization}}$ = 9.05 kcal/mol and density = 0.759 gm/cm^3.) The contributions to the molecular dipole moment are presented in Table 6; the induced moments are essentially along the molecular axis, giving rise to the higher total average moment. The variation of the magnitude of the induced moments is striking; liquid methanol obviously corresponds to a very "heterogeneous environment". The diffusion constant (Figure 8) for the additive model is too high, whereas the polarizable model gives a reasonable value of 0.265×10^{-8} m^2/s *vs* 0.22×10^{-8} m^2/s found experimentally.[20]

The number of hydrogen bonds formed by each monomer can vary from one (as in a gas phase dimer) to two in a perfect crystal.[26] The values deduced from experiment range from 2 to ~1.5[27] on the basis of the RDF of the O–O distance. The difficulty in determining a value from the experimental RDFs is the onset of the C–O curve at about 2.8 Å. The published experimental RDF[28] is only available in analog form, so we merely note that the first peak is at 2.8 Å with a height of ~1.2 followed by broader peaks at 3.8 and 4.5 Å. Since the first two peaks overlap strongly, it is difficult to integrate the area

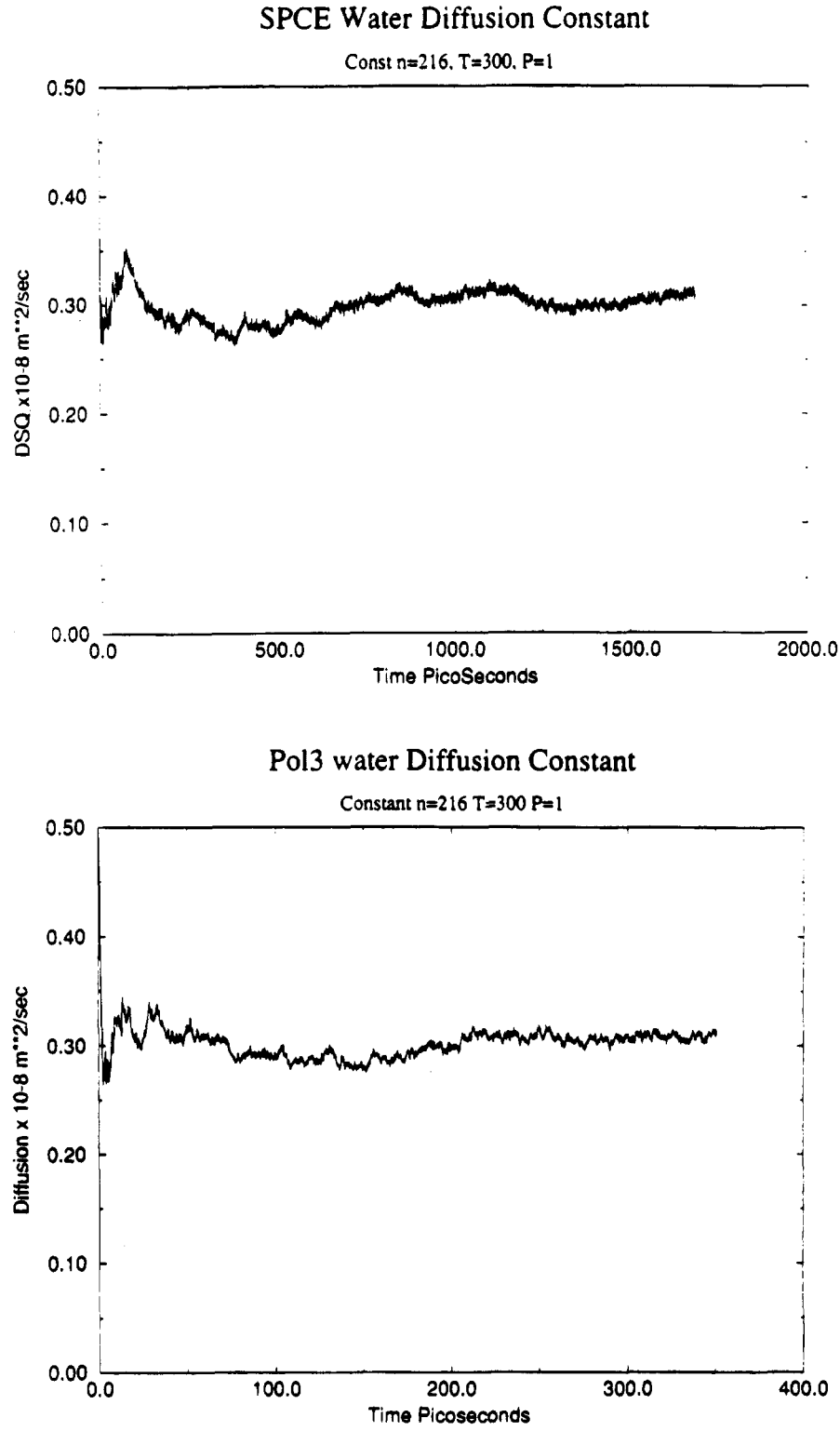

Figure 5. Water: calculated diffusion coefficients (T = 300 K, P = 1 bar, 216 molecules/box).

under the first curve cleanly, but Narten and Habenschuss[27] claim the area corresponds to 1.8 hydrogen bonds/molecule. Jorgensen came up with a similar value.[24b]

We integrated the area under the first peak of the RDF curves and obtained a value of ~1.3 for each of the nonadditive and additive models for both the O−O (Figure 4) and O−H curves (not shown). We generated a graphics image of the polarized model where "hydrogen bonds" were displayed for H···O distances of less than 2.2 Å. It was seen that while most of the methanol molecules are involved in hydrogen bonds (64 hydrogen bonds), only a few participate in short chains. This is, of course, only a snapshot of the system, whereas the RDFs are the average of 25 000 MD steps; however, our results suggest that methanol is significantly less organized than 1.8 hydrogen bonds/molecule. (No image is presented here, as there is no adequate way to display 125 molecules as pseudo-3D in only 2D.)

We produced a "pseudoexperimental" RDF by adding the OO, CO, and CC RDFs together to test the sensitivity of the integration choices, Figure 9. There mere shift of the upper integration limit of the first peak from 3.2 to 3.4 Å results in a change from 1.4 to 1.9 hydrogen bonds/molecule. Our model

TABLE 4: Average Quadrupole Moments[a,b]

	θ_{xx}	θ_{yy}	θ_{zz}
	Water		
SPC/E	−1.40	−0.22	1.63
POL3			
permanent charges	−1.21	−0.19	1.40
total	−1.05	−0.29	1.34
q.m.[c]	−1.80	−0.08	1.88
	MEOH		
additive model	−1.64	−1.15	2.79
polarizable model			
permanent charges	−1.41	−0.93	2.33
total	−1.26	−0.79	2.05
q.m.[d]	−1.99	−0.89	2.86
	NMA		
additive model	−3.84	−0.54	4.37
polarizable model			
permanent charges	−3.37	−0.37	3.74
total	−3.35	−0.31	3.66
q.m.[d]	−3.41	−0.59	3.99

[a] Atomic units. [b] All molecules aligned by principal axis transformation to the same axes. [c] Reference 21. [d] 6-31G*//6-31G* using Gaussian92.[19]

suggests that the actual number of hydrogen bonds/molecules is in the 1.3−1.4 range.

The quadrupole moment for the additive model actually comes much closer to the quantum mechanical value (Table 4) than the value from the nonadditive calculation. The origin of the net reduction of the quadrupole moment due to the induced dipoles is not clear.

***N*-Methylacetamide.** Jorgensen has also studied dimeric and liquid NMA.[28] That work found the preferred orientation for dimers parallel or antiparallel with respect to the C−N bond. The current models (both additive and nonadditive) have the C−C bonds "orthogonal" to each other apparently to avoid steric interaction between the methyl groups (Figure 10).

The energetics for liquid and dimeric NMA are shown in Table 7. NMA is treated as consisting of 100% *trans* molecules,

TABLE 5: Methanol Properties (T = 300 K, P = 1 bar)

	density[a]	ΔH^b	ΔE^b
	Liquid		
exptl	0.79	8.94	
OPLS	0.76	9.05	
Add	0.78	8.6	8.1
q88	0.81	8.5	8.0
q90	0.82	9.1	8.7
Add_lr[c]	0.82	9.0	8.6
q88_lr[c]	0.835	8.8	8.4

	model		
	Add	q88	q90
	Monomer[e]		
$E_{\text{minimized}}$[b,d]	5.3	3.8	4.0
$E_{\text{vibration}}$[b,e]	1.99	1.99	1.99
	Dimer		
$E_{\text{minimized}}$[b,d]	3.9	1.9	2.0
ΔE[f]	6.4	5.7	6.0
geometry[g]			
R_{O-O}	2.78	2.79	2.76
R_{O-H}	1.82	1.83	1.80

[a] gm/cm^3. [b] kcal/mol. [c] Long-range correction for effect of molecules outside the spherical cutoff (ref 27) included in the Hamiltonian. [d] Static molecular mechanical energy in kcal/mol. [e] Thermal energy of a monomer in kcal/mol. [f] Dimerization energy. [g] Å.

TABLE 6: Magnitude of Induced Moments on Atoms of MEOH[a] for q88 (D)

atom	ave	max	min
C1	0.10	0.30	0.02
HC1	0.09	0.31	0.03
HC2	0.10	0.32	0.01
HC3	0.10	0.32	0.01
O1	0.10	0.30	0.01
HO1	0.10	0.26	0.03
methyl[b]	0.25		
O−H[b]	0.18		

[a] The average angle between permanent and induced moments ~20°. [b] Vector sum over the induced moments.

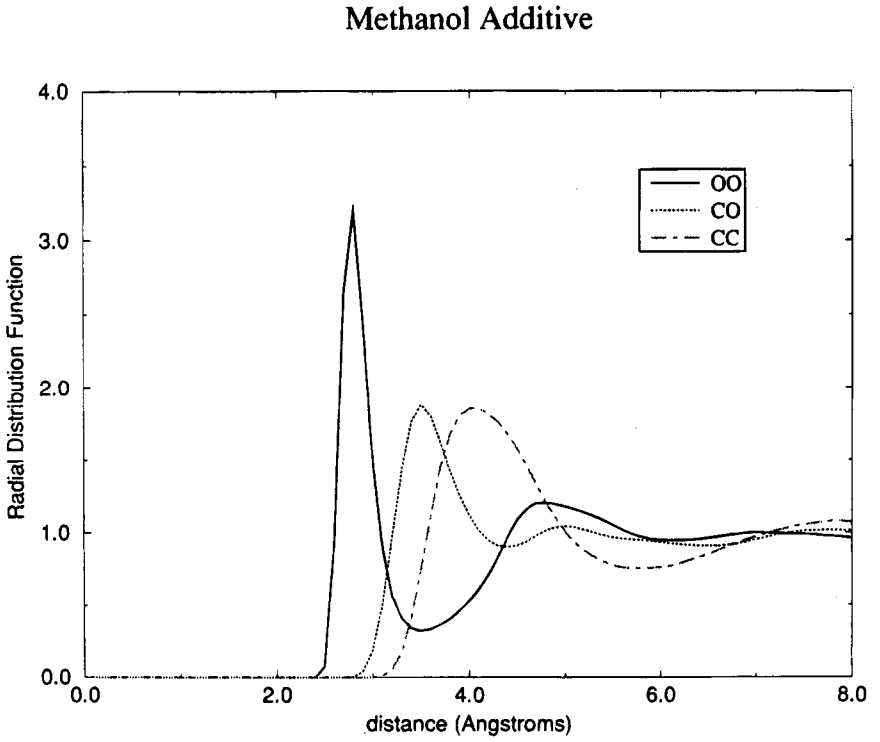

Figure 6. Methanol: additive potential radial distribution functions (T = 300 K, P = 1 bar, 125 molecules/box, >20 000 step average).

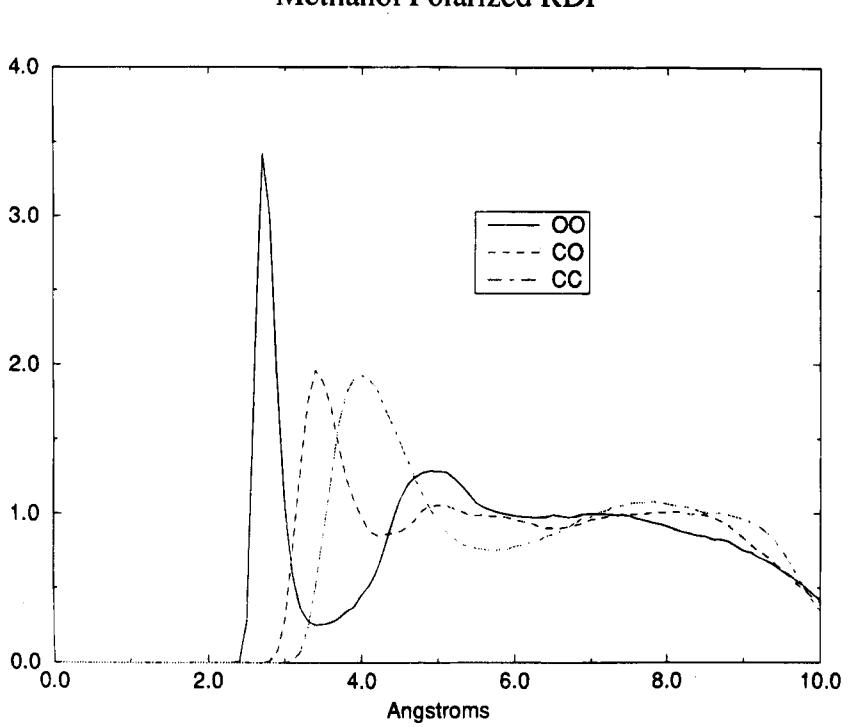

Figure 7. Methanol: nonadditive potential radial distribution functions (T = 300 K, P = 1 bar, 125 molecules/box, >10 000 step average).

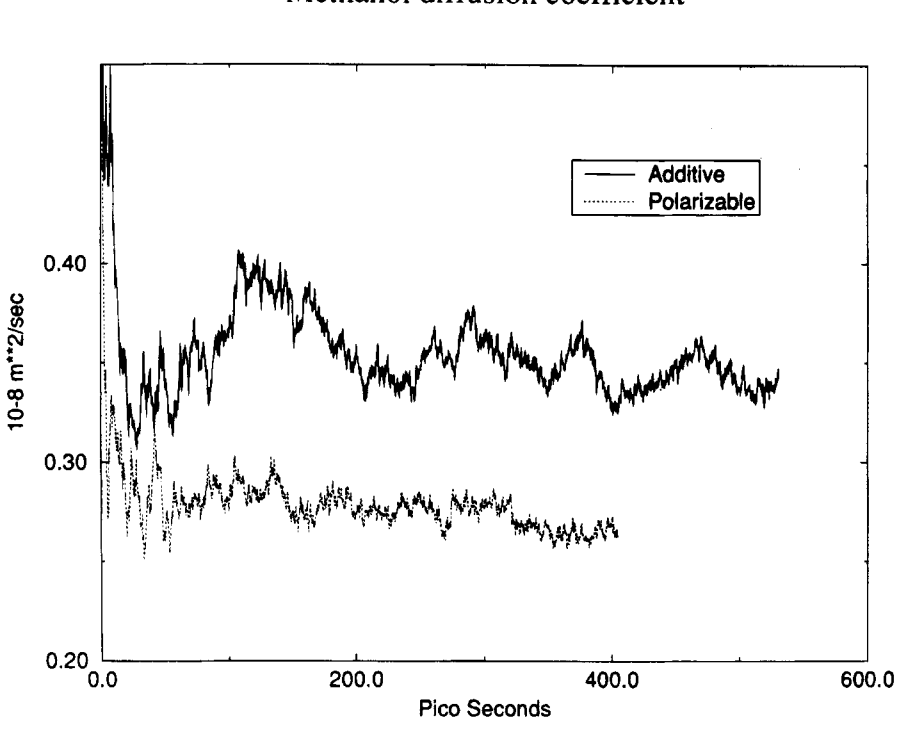

Figure 8. Methanol: calculated diffusion coefficients (T = 300 K, P = 1 bar, 125 molecules/box).

whereas there is a small fraction (~3%) of *cis* molecules found experimentally in the gas phase.[29] The experimental density, enthalpy of vaporization, and diffusion constant of the liquid are from Lemire and Sears.[30] After simulations of >200 ps each, the differences in calculated density and enthalpy of vaporization are very similar for the 0.90 and 0.88 (Table 7) scale factors. We choose to use 0.88 because that yields marginally better values than 0.90 and, more importantly, is the same as the preferred value for methanol. The agreement with the experimental values is good. Two things are interesting to note about the NMA dipole moments: (1) in the monomer, the induced moment reduces the total moment and (2) the net dipole moment of polarizable liquid NMA is enhanced compared to the gas phase due to the induced moment no longer opposing the fixed moment. This comes about due to the average orientation of the induced moment (0.46 D) being nearly perpendicular (90.3°) to the permanent moment in the liquid (the induced moment is nearly parallel to the permanent moment in both water (~19°) and methanol (~20°)). The induced moments presented in Table 8 provide an insight as to why

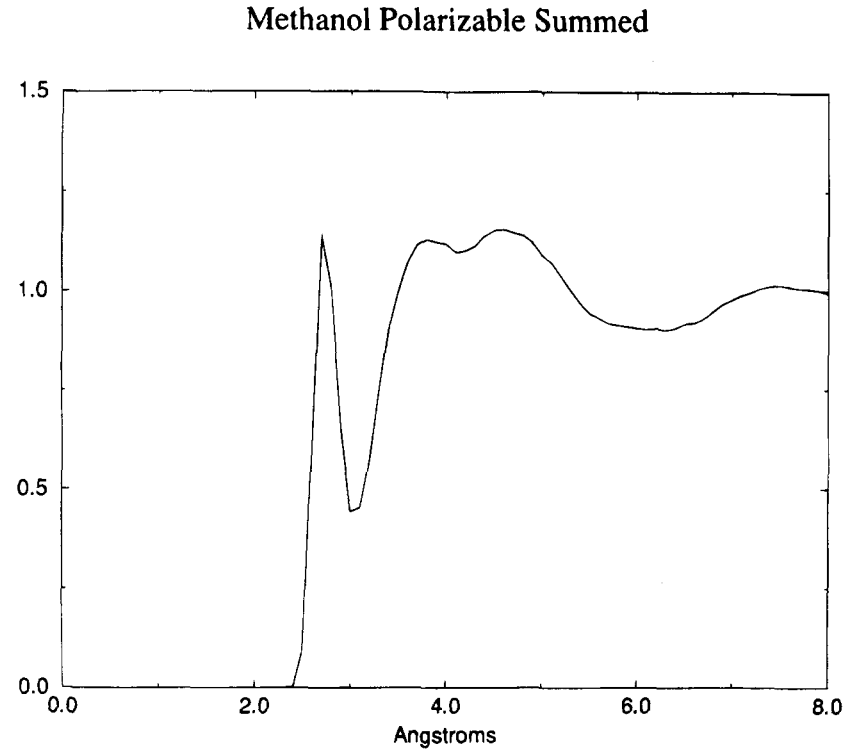

Figure 9. Methanol: summation of radial distribution functions with nonadditive potential.

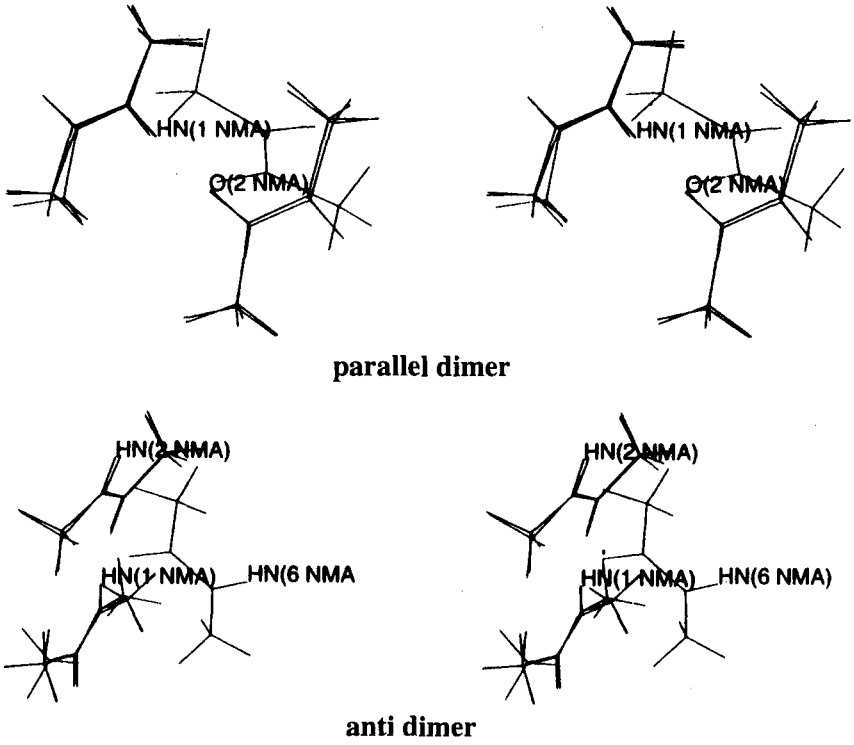

Figure 10. Stereoviews of *N*-methylacetamide: dimer structures (Atoms C, O, N, HN of residue 1 of the pairs [1/2, 3/4, 5/6] were superimposed. Residues 1,2 are the model-built structure based on Figure 2 in ref 25; residues 3,4 are minimized; residues 5,6 are the result of minimization, dynamics for 10 ps at 300 K, and reminimization).

this is the case, in that the largest contributions come from the methyl groups oriented perpendicular to the molecular axis.

A notable difference between MEOH and NMA is the magnitude of the induced moments on the atoms (although the range is similar). For MEOH, all of the atoms have nearly the same induced moments, whereas for NMA the hydrogens of the methyl groups are only half as polarized as the other atoms. This is evidently the origin of the difference in orientation of the induced moments to the permanent moments.

The quadrupole moment (Table 4) is in good agreement with the quantum mechanical value. Interestingly, the induced moments charge the value very little (compared to water and MEOH).

There are no experimental RDFs for NMA, but Jorgensen has calculated them for the OPLS parameter model.[29] The current RDFs are shown in Figures 11 and 12; they closely follow the ones obtained by Jorgensen.

The diffusion constant, however, is rather too high for both

TABLE 7: *N*-Methylacetamide Properties (T = 373 K, P = 1 bar)

	density[a]	ΔH^b	ΔE^b
	Liquid		
exptl	0.89	13.3	
OPLS	0.87	13.2	12.4
Add	0.87	13.8	13.0
q88	0.87	12.5	11.7
q90	0.87	12.7	11.9
Add_lr[c]	0.90	14.4	13.6
q88_lr[c]	0.89	12.5	11.7
	Add	q88	q90
	Monomer[d]		
$E_{minimized}$	1.23	−0.37	−0.45
$E_{vibrational}$[e]	6.73	6.73	6.73
	Dimer[f]		
$E_{minimized}$	−7.19	−9.03	−9.41
ΔE[g]	9.65	8.29	8.51
geometry[h]			
R_{O-N}	2.86	2.86	2.87
R_{O-HN}	1.89	1.88	1.90

[a] gm/cm³. [b] kcal/mol. [c] Long-range correction for effect of molecules outside the spherical cutoff (ref 27) included in the Hamiltonian. [d] Static molecular mechanical energy in kcal/mol. [e] Thermal energy of monomer. [f] Static molecular mechanical energy in kcal/mol. [g] Dimerization energy. [h] Å.

TABLE 8: Induced Moments on Atoms and Groups of *N*-Methylacetamide q88 (D)[a]

	Atoms		
	ave	max	min
C1	0.14	0.28	0.03
H1	0.05	0.07	0.02
H2	0.05	0.08	0.02
H3	0.09	0.19	0.03
C	0.12	0.23	0.02
O	0.07	0.17	0.01
N	0.09	0.17	0.01
HN	0.12	0.33	0.02
C2	0.20	0.34	0.04
H4	0.03	0.06	0.01
H5	0.03	0.05	0.01
H6	0.09	0.28	0.02
	Groups[b]		
Me1			0.16
C−O			0.13
N−H			0.14
Me2			0.21
peptide unit			0.19

[a] The average angle between permanent and induced moments ~90°. [b] Vector sum over the induced moments.

the additive (0.18×10^{-8} m²/s) and polarizable models (0.27×10^{-8} m²/s) (Figure 13). The experimental value[26] would be $\sim 0.12 \times 10^{-8}$ m²/s by extrapolating from data determined at 308 K and 333−373 K.

"Turning on" the OPLS type long-range correction (ref 31, eqs 2.136, 2.137, and 2.138) produced only a small effect for the MEOH and NMA systems, as shown in Tables 5 and 7 (water was run as a control, and the results were, as expected, identical with the standard approach). In MEOH, there was a 2−4% increase in the density and a 3−4% change in the enthalpy of vaporization; in NMA the density increased by 2−3% and the enthalpy of vaporization increased for the additive model by ~4%. For MEOH, the long-range correction improved the agreement with experiment for the enthalpy of vaporization and worsened it for the density; in NMA, the density with the long-range correction was improved for both models, but the enthalpy was unaffected (nonadditive) or the agreement was worsened (additive).

Discussion and Conclusions

The calculations presented here show encouraging agreement with both experiment and the OPLS method. It is gratifying

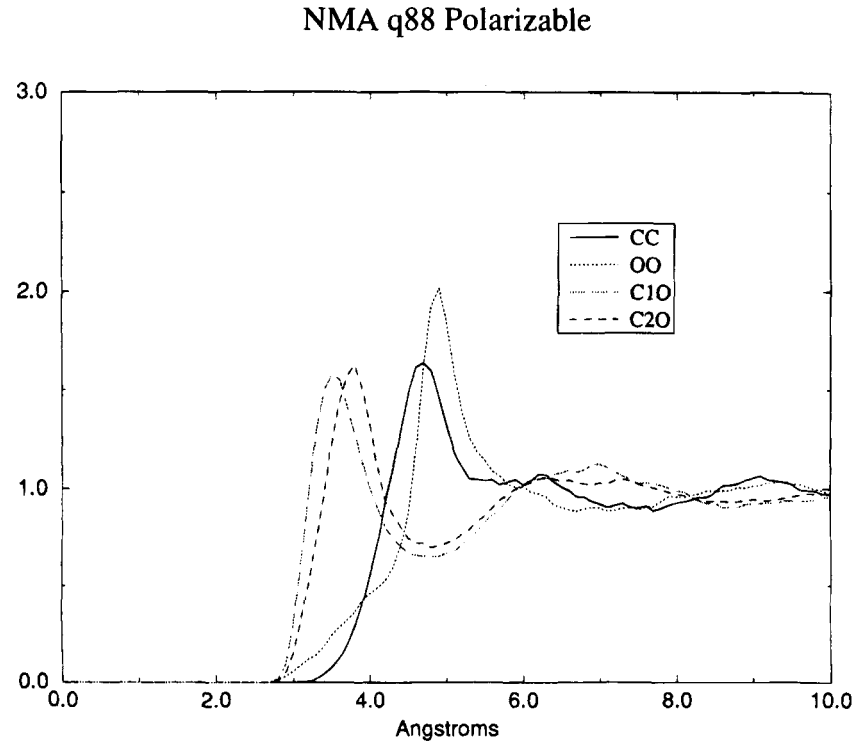

Figure 11. *N*-Methylacetamide: nonadditive radial distribution functions for CC, OO, O−CH_3N (C2O), and O−CH_3C (C1O) (T = 373 K, P = 1 bar, 125 molecules/box, >10 000 step average).

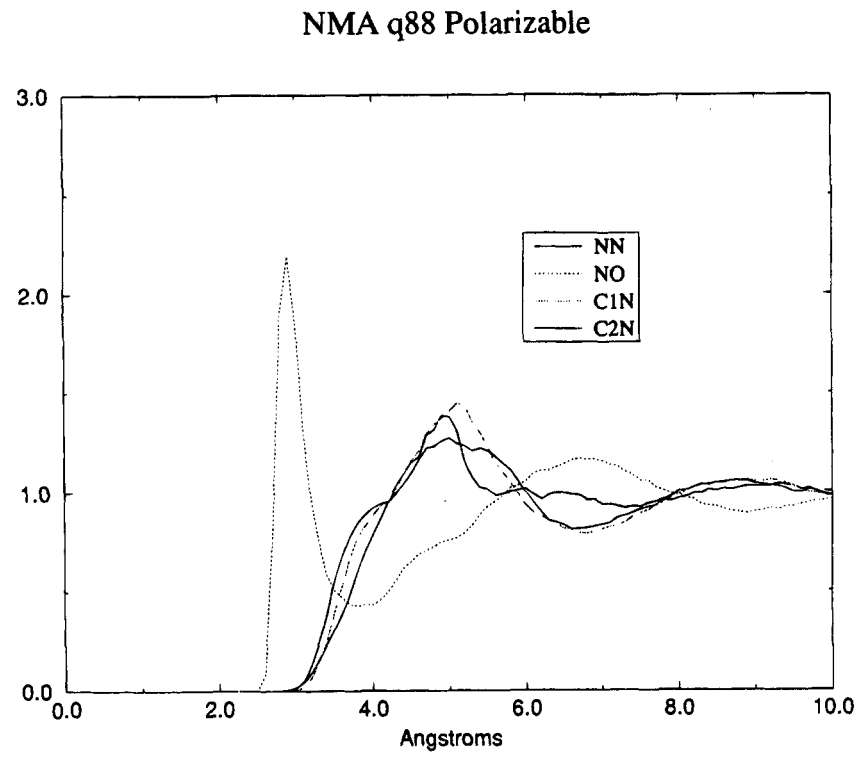

Figure 12. *N*-Methylacetamide: nonadditive radial distribution functions for NN, NO, N−CH_3N (C2O), and N−CH_3C (ClO) (T = 373 K, P = 1 bar, 125 molecules/box, >10 000 step average).

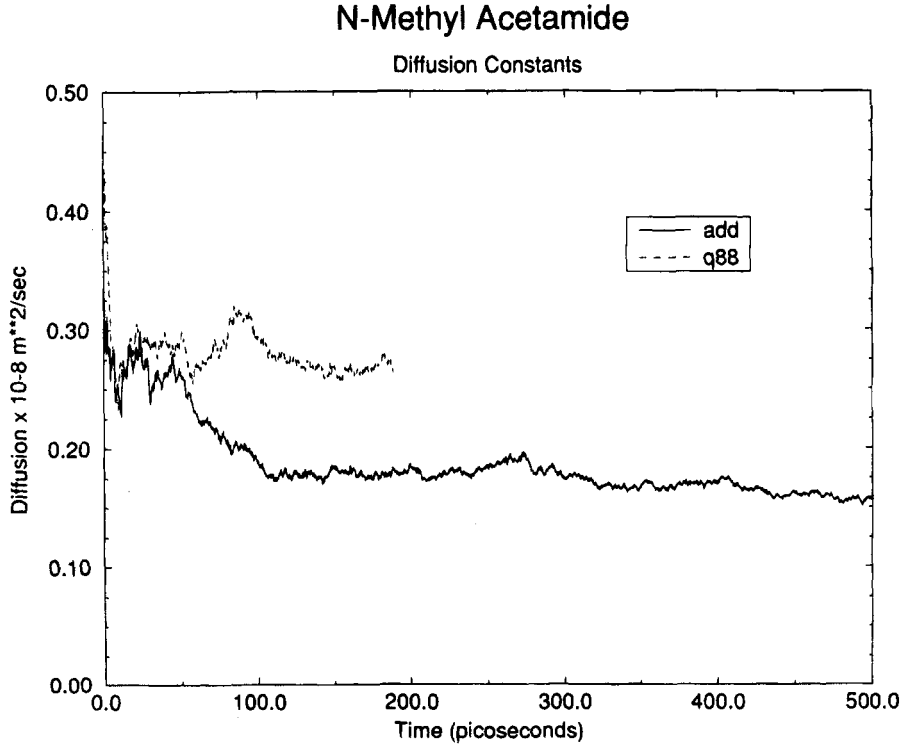

Figure 13. *N*-Methylacetamide: calculated diffusion coefficients (T = 373 K, P = 1 bar, 125 molecules/box).

that the additive models of methanol and NMA liquid have been taken without change from previous studies of aqueous solvation free energies on these molecules. Thus, it is particularly encouraging that the densities of the liquids are within 3% (MEOH) and 1% (NMA) and the vaporization enthalpies within 1% (MEOH) and 8% (NMA) of experiment. For the nonadditive model, we found that a single scale factor for the permanent charge of 0.88 and the inclusion of induction energies allow a comparably accurate representation of the enthalpy and density of the vaporization of the liquids.

This scale factor of 0.88 is also encouragingly close to the 0.86 found by us to be appropriate to "transform" SPC/E water into POL water (refs 11a, 12c, and this work). It is of note that even with this scaling of the charges, the intrinsic gas phase monomer dipole moments are 6−12% larger than experiment (Table 2). This is not unreasonable, give the *underestimate* of

the quadrupole moment of H_2O inherent in atom-centered charge models, that the dipole moment should be slightly *overestimated* to provide an appropriately balanced charge model.

The calculated diffusion constants all are higher than experimental values, though generally not by a large amount, with the exception of the methanol additive value. There is no obvious correlation between the diffusion constants and deviations of enthalpy of vaporization and density *vs* experiment.

It is very difficult to unambiguously analyze the experimental radial distributions (our simple attempts to do such brought clearly home the delicacy of such attempts). In this case, it is especially noteworthy that the combined calculated RDF for methanol showed such nice agreement with experiment, even though our interpretation was sharply different from the previous ones. It is likely that, although there are transient "macrostructures" in liquid methanol, the average structure is less organized than previously suggested.

A particular benefit of the nonadditive method is the insight it gives into the nature of induced moments in liquids via the range and average magnitudes of the induced moments. It is quite unexpected that the induced moment of NMA is nearly perpendicular to the "permanent" moment, whereas that of methanol reinforces the permanent moment. Thus, a simple additive model of NMA may not adequately describe the orientations of interacting molecules.

This work shows that the simple approach of adding induced polarizabilities to a reliable additive molecular mechanical force field can provide valuable insight and a clearly understandable improvement of the microscopic electric properties which will be necessary to understand interesting highly charged enzyme reaction systems such as proteins.

Acknowledgment. We would like to thank Digital Equipment Corporation for the Grant of the Alpha 3000/500. P.A.K. also thanks the NIH and NSF for support (GM-29072 and CHE 91-13472). We would also like to thank a referee for pointing out the best value of the water self-diffusion constant.

References and Notes

(1) (a) Jorgensen, W. L.; Tirado-Rives, J. *J. Am. Chem. Soc.* **1988**, *110*, 1657. (b) Jorgensen, W. L.; Briggs, J. M. *J. Am. Chem. Soc.* **1989**, *111*, 4190. (c) Jorgensen, W. L.; Briggs, J. M.; Contreras, M. L. *J. Phys. Chem.* **1990**, *94*, 1683.

(2) (a) Weiner, S. J.; Kollman, P. A.; Case, D. A.; Singh, U. C.; Ghio, C.; Alagona, G.; Pofeta, S.; Weiner, P. *J. Am. Chem. Soc.* **1984**, *106*, 765. (b) Weiner, S. J.; Kollman, P. A.; Nguyen, D. T.; Case, D. A. *J. Comput. Chem.* **1986**, *7*, 230–252.

(3) Cornell, W. D.; Cieplak, P.; Kollman, P. A. *J. Am. Chem. Soc.*, in press.

(4) Sun, Y.; Spellmeyer, D.; Pearlman, D. A.; Kollman, P. A. *J. Am. Chem. Soc.* **1992**, *114*, 6798–6801.

(5) Gough, C. A.; Debolt, S. E.; Kollman, P. A. *J. Comput. Chem.* **1992**, *13*, 963–970.

(6) Singh, U. C.; Kollman, P. A. *J. Comput. Chem.* **1984**, *5*, 129–145.

(7) Cieplak, P.; Kollman, P. A. *J. Comput. Chem.* **1991**, *12*, 1232–1236.

(8) Kuyper, L. F.; Hunter, R. N.; Ashton, D.; Merz, K. M.; Kollman, P. A. *J. Phys. Chem.* **1991**, *95*, 6661–6666.

(9) Bayly, C. I.; Cieplak, P.; Cornell, W. D.; Kollman, P. A. *J. Phys. Chem.* **1993**, *97*, 10269–10280.

(10) Cornell, W. D.; Cieplak, P.; Bayly, C. I.; Kollman, P. A. *J. Am. Chem. Soc.* **1993**, *115*, 9620–9631.

(11) (a) Caldwell, J. W.; Dang, L. X.; Kollman, P. A. *J. Am. Chem. Soc.* **1991**, *112*, 9144–9147. (b) Dang, L. X.; Rice, J. E.; Caldwell, J. W.; Kollman, P. A. *J. Am. Chem. Soc.* **1991**, *113*, 2481–2486.

(12) (a) Ahlstrom, P.; Wallquist, A.; Engstrom, S.; Jonsson, B. *Mol. Phys.* **1989**, *68*, 563–581. (b) Bernardo, D. N.; Ding, Y. B.; Krough-Jespersen, K.; Levy, R. M. *J. Phys. Chem.* **1994**, *98*, 4180–4187. (c) Dang, L. X. *J. Chem. Phys.* **1992**, *97*, 2659–2660. (d) Sprik, M.; Klein, M. L. *J. Chem. Phys.* **1988**, *89*, 7556–7560. (e) Rick, S. E.; Stuart, S. J.; Berne, B. J. *J. Chem. Phys.* **1994**, *101*, 6141–6156.

(13) Applequist, J. B.; Carl, J. R.; Fung, K.-K. *J. Am. Chem. Soc.* **1972**, *94*, 2952–2960.

(14) Thole, B. T. *Chem. Phys.* **1981**, *59*, 341–350.

(15) Jorgensen, W. L.; Chandrasekhar, J.; Madura, J. D.; Impey, R. W.; Klein, M. L. *J. Chem. Phys.* **1983**, *79*, 926–935.

(16) Berendsen, H. J. C.; Postma, J. P. M.; van Gunsteren, W. F., DiNola, A.; Haak, J. R. *J. Chem. Phys.* **1984**, *81*, 3684–3690.

(17) Ryckaert, J.; Cioccotti, G.; Berendsen, H. J. C. *J. Comput. Phys.* **1977**, *23*, 327–341.

(18) Berendsen, H. J. C.; Grigera, J. R.; Straatsma, T. P. *J. Phys. Chem.* **1987**, *91*, 6269–6271.

(19) Frisch, M. J.; Trucks, G. W.; Head-Gordon, M.; Gill, P. M. W.; Wong, M. W.; Foresman, J. B.; Johnson, B. G.; Schlegel, H. B.; Robb, M. A.; Replogle, E. S.; Gomperts, R.; Andres, J. L.; Raghavachari, K.; Binkley, J. S.; Gonzalez, C.; Martin, R. L.; Fox, D. J.; Defrees, D. J.; Baker, J.; Stewart, J. J. P.; Pople, J. A. *Gaussian 92*, Revision C.4; Gaussian, Inc.: Pittsburgh, PA, 1992.

(20) Krynicki, K.; Green, C. D.; Sawyer, D. W. *Faraday Discuss. Chem. Soc.* **1978**, *66*, 199–209.

(21) Coulson, C.; Eisenberg, D. *Proc. R. Soc. London, A* **1966**, *291*, 445.

(22) Soper, A. K.; Phillips, M. G. *Chem. Phys.* **1986**, *107*, 47–60.

(23) Neumann, D.; Moscowitz, J. W. *J. Chem. Phys.* **1968**, *49*, 2056–2070.

(24) (a) Jorgensen, W. L.; Tirado-Rives, J. *J. Am. Chem. Soc.* **1988**, *110*, 1657–1661. (b) Jorgensen, W. L. *J. Phys. Chem.* **1986**, *90*, 1276–1284.

(25) (a) Wilholt, R. C.; Zwolinski, B. J. *J. Phys. Chem. Ref. Data* **1973**, *2*, Suppl. 1. (b) Lee, Y. E.; Li, S. F. M. *J. Chem. Eng. Data* **1991**, *36*, 240–243.

(26) Tauer, K. J.; Lipscomb, W. N. *Acta Crystallogr.* **1952**, *6*, 606.

(27) (a) Narten, A. H.; Habenschuss, A. *J. Chem. Phys.* **1984**, *80*, 3387–3391. (b) Magini, M.; Paschina, G.; Piccaluga, G. *J. Chem. Phys.* **1982**, *77*, 2051–2056. (c) Sarkar, S.; Joarder, S. N. *J. Chem. Phys.* **1993**, *99*, 2033–2039.

(28) Jorgensen, W. L.; Swenson, C. J. *J. Am. Chem. Soc.* **1985**, *107*, 569–578.

(29) (a) Drakenberg, T.; Forsen, S. *J. Chem. Soc., Chem. Commun.* **1977**, 1404. (b) Neuman, R. C.; Jonas, V.; Anderson, K.; Barry, R. *Biochem. Biophys. Res. Commun.* **1971**, *44*, 1156. (c) Drakenberg, T.; Dahlqvist, K.-I.; Forsen, S. *J. Chem. Phys.* **1972**, *76*, 2178.

(30) Lemire, R. J.; Sears, P. G. *Top. Curr. Chem.* **1978**, *74*, 45–91.

(31) Allen, M. P.; Tildesley, D. J. *Computer Simulations of Liquids*; Oxford University Press: Oxford, Great Britain, 1987; pp 64–65.

JP942675S